# Test-retest reproducibility of [11C]PBR28 binding to TSPO in healthy control subjects.

**Collste K, Forsberg A, Varrone A, Amini N, Aeinehband S, Yakushev I, Halldin C, Farde L, Cervenka S.**

Department of Clinical Neuroscience, Centre for Psychiatry Research, Karolinska Institutet, Stockholm, Sweden,

Corresponding author: karin.collste@ki.se.

Published in: Eur J Nucl Med Mol Imaging. 2015 Aug 22
Doi: 10.1007/s00259-015-3149-8

# Test-retest reproducibility of [$^{11}$C]PBR28 binding to TSPO in healthy control subjects.

Collste K [1], Forsberg A [1], Varrone A [1], Amini N [1], Aeinehband S [2], Yakushev, I [1,3], Halldin C [1], Farde L [1], Cervenka S [1]

[1]Karolinska Institutet, Department of Clinical Neuroscience, Centre for Psychiatry Research, Stockholm, Sweden

[2]Karolinska Institutet, Department of Clinical Neuroscience, Neuroimmunology Unit, Stockholm, Sweden

[3]Dept. of Nuclear Medicine, b. TUM Neuroimaging Center (TUM-NIC), Technische Universität München, Munich, Germany

## Abstract

*Purpose*

The PET radioligand [$^{11}$C]PBR28 binds to the translocator protein (TSPO), a marker for brain immune activation. Here, we examined reproducibility of [$^{11}$C]PBR28 binding in healthy subjects as quantified on a regional and voxel-by-voxel basis. In addition, a preliminary analysis of diurnal changes in TSPO availability was performed.

*Methods*

Twelve subjects were examined with HRRT PET and [$^{11}$C]PBR28, six in the morning and afternoon on the same day, and six in the morning of two separate days. Regional Volume of distribution ($V_T$) values were derived using a region-of-interest based two-tissue compartmental analysis (2TCM), as well as a parametric approach. Metabolite-corrected arterial plasma was used as input function.

*Results*

For the whole sample, the mean absolute variability of $V_T$ in gray matter (GM) was 18.3 ± 12.7 %. Intraclass Correlation Coefficient values in GM regions ranged from 0.90 to 0.94. Reducing the time of analysis from 91 to 63 minutes yielded a variability of 16.9 ± 14.9%. There was a strong correlation between the parametric and 2TCM-derived GM values (r=0.99). A significant increase in GM $V_T$ was observed between morning and afternoon examinations when using secondary methods of quantification (p=0.028). For the subjects examined at the same time of the day, the absolute variability was 15.9 ± 12.2 % for the 91 minute 2TCM data.

*Conclusions*

$V_T$ of [$^{11}$C]PBR28 binding showed medium reproducibility and high reliability in GM regions. Our findings support the use of parametric approaches for determining [$^{11}$C]PBR28 $V_T$ values, and indicate that the acquisition time could be shortened. Diurnal changes in TSPO binding in brain may be a potential confounder in clinical studies and has to be investigated further.

## Keywords

[$^{11}$C]PBR28; PET; Brain imaging; Test-retest

## Background

The immune surveillance system in brain is thought to play a role in the pathogenesis of a number of severe medical conditions, including Multiple Sclerosis, Parkinson's disease, Alzheimer's disease as well as psychiatric disorders such as Schizophrenia. The development of methodology to examine immune activation in brain is

thus of central interest in research on CNS-disorders. Microglia cells are considered the resident macrophages of the brain, responsible for the phagocytosis of cellular debris, antigen presentation and a variety of other functions including cytokine signalling [1,2].

Microglia cells express the translocator protein (TSPO), an intracellular protein formerly known as the peripheral benzodiazepine receptor [3]. With molecular imaging techniques, such as Positron Emission Tomography (PET), it is possible to measure TSPO levels in the brain. [$^{11}$C]PK 11195 is to date the most widely used radioligand for that purpose [4]. However, this radioligand has some disadvantages, such as low specific to non-specific binding ratio [5]. In addition, a recent test-retest study in control subjects showed only moderate intraindividual reproducibility in [$^{11}$C]PK11195 binding [6], as compared to commonly used neuroreceptor radioligands such as [$^{11}$C]raclopride [7]. More recently, several novel TSPO radioligands with improved characteristics have been developed [8]. Of those, [$^{11}$C]PBR28, is a promising candidate which, in a comparison with [$^{11}$C]PK11195, shows higher specific binding and better kinetic properties [5,9,10].

[$^{11}$C]PBR28 has been used to show changes of TSPO binding in an increasing number of clinical studies [11–14]. However, information on the test-retest reproducibility of [$^{11}$C]PBR28 binding has not yet been published, limiting the interpretation of clinical research.

The primary aim of this PET study was to examine the reproducibility of [$^{11}$C]PBR28 binding in healthy control subjects. A secondary aim was to compare the standard ROI-based compartmental analysis to a parametric approach for quantification of [$^{11}$C]PBR28 binding. Moreover, in a preliminary analysis of diurnal changes in TSPO binding [15,16], the study was designed so that six subjects were examined in the morning and afternoon on the same day, and six subjects at the same time point on two different days.

## Methods

### Subjects

The study was conducted at the Karolinska University Hospital, Solna, Sweden and was approved by the regional Ethics Committee in Stockholm and the Radiation Safety Committee at the Karolinska University Hospital, Stockholm.

Subjects were recruited by advertisement and provided written informed consent. They were healthy according to medical history, clinical examination and routine laboratory tests in blood and urine. All subjects were assessed by a senior psychiatrist (K.C.), using the Mini International Neuropsychiatric Interview (MINI) for psychiatric diagnoses. None of the subjects had previously been exposed to psychopharmacological medication. Furthermore, a negative illegal drug screening test was ascertained in all subjects, prior to PET examination. None of the subjects were on any medication at the time of the study. No brain abnormality was detected on magnetic resonance imaging (MRI), as evaluated by a neuroradiologist at the MR-centre, Karolinska University Hospital, Solna.

As demonstrated both *in vitro* and *in vivo*, [$^{11}$C]PBR28 binding is influenced by an identified single point mutation in the TSPO gene [8,17]. At screening, a blood sample was collected and genotyping was performed according to the description below. In total, 15 subjects were recruited. Of these, one was a low affinity binder (LAB) and was therefore excluded from the analysis. Two additional subjects were excluded due to technical issues with the PET measurements. The remaining twelve subjects were six men and six women, with a mean age of 23.9 SD ± 3.1 years. Six were high affinity binders (HABs) and six were mixed affinity binders (MABs).

### Study design

Six subjects were examined with PET in the morning and in the afternoon on the same day and six in the morning of two separate days, 2-5 days apart. Both gender and binding affinity were equally distributed in the two groups. For the individuals examined twice on the same day, the average interval between measurements

was 3 hours and 25 minutes. For the group examined on two different days, the mean interval was 3.3 days, and the mean difference between injection times was 20 minutes.

## Genotyping

TSPO genotype was assessed using a Taqman based polymerase chain reaction (Applied Biosystems® QuantStudio™ 7) assay specific for the rs6971 polymorphism (Applied Biosystems, C_2512465_20, cat.# 4351379) in the TSPO gene. In brief, genomic DNA was extracted from 8 ml of whole blood (QIAamp® DNA Blood Maxi) and DNA was diluted in DNase-free water before the test, to give a final amount of 20 ng/well. Each DNA sample was plated and mixed with 2X TaqMan Genotyping mix (Applied Biosystems) in a 384-well microtiter plate (MicroAmp Optical 384-well reaction plate, Applied Biosystems) to a final reaction volume of 5 µl. The DNA extraction and Taqman PCR were performed according to the manufacturer's instructions.

## Magnetic resonance imaging

Brain magnetic resonance imaging was performed using a 3 Tesla General Electric Discovery MR750 system (GE, Milwaukee, WI, USA). T2-weighted images were acquired for clinical evaluation regarding pathology, and T1-weighted images were acquired for co-registration with PET and definition of anatomical brain regions.

## Radiochemistry

The method used for radiosynthesis was modified from the work by Briard and co-workers [18]. Briefly, [$^{11}$C]PBR28 was produced by [$^{11}$C]methylation of the salt formed from desmethyl PBR28 and tetrabutylammonium hydroxide in MeOH (1.0 M, QOH) in acetone at room temperature. The product is purified by semi-preparative HPLC, isolated and formulated in phosphate buffered saline (pH = 7.4) containing less than 10% ethanol.

## Positron emission tomography procedures

PET measurements were performed at the PET centre at Karolinska Institutet, Stockholm. Individualized plastic helmets were made for each subject and used with a head fixation system, to minimize movement artefacts and to reproduce the head positioning in each examination [19]. The subjects were placed recumbent with the head in the PET system. A cannula was inserted into the left radial artery and another one into the right cubital vein. A sterile phosphate buffer (pH = 7.4) containing radioligand was injected as a bolus over 10 seconds into the cubital vein. The cannula was then immediately flushed with a 10 mL saline solution.

PET measurements were conducted using the High Resolution Research Tomograph (Siemens Molecular Imaging, Knoxville, TN, USA). The axial field of view is 25.2 cm, corresponding to 207 planes in the reconstructed images, with a pixel size of 1.218×1.218×1.218 mm$^3$. Attenuation correction was acquired with a 6 min transmission measurement using a single $^{137}$Cs source. Brain radioactivity was acquired in a consecutive series of time frames for up to 91 min, except for one individual, where the acquisition time was 60 minutes, due to technical problems. List mode data were reconstructed using the ordinary Poisson-3D-ordered subset expectation maximization algorithm, with 10 iterations and 16 subsets including modelling of the point spread function. The corresponding in-plane resolution with ordinary Poisson-3D-ordered subset expectation maximization point spread function was 1.5 mm in the centre of the field of view and 2.4 mm at 10-cm off-centre directions [20].

## Arterial blood sampling

An automated blood sampling system (ABSS) was used during the first five minutes of each PET measurement [21]. After that, arterial blood samples (1-3 mL) were drawn manually at 1, 3, 5, 7, 9, 10.5, 20, 30, 40, 50, 60, 70, 80 and 90 minutes. The radioactivity was measured immediately afterwards in a well counter, cross-calibrated with the PET-system. After centrifugation, 0.8-1.5 mL plasma was pipetted and radioactivity was measured in the same well counter.

## Radiometabolite and plasma protein binding analysis

A reversed-phase HPLC method was used to determine the percentages of radioactivity in plasma that corresponded to unchanged radioligand and radiometabolites during the course of each PET measurement. The plasma (0.7-1.5 mL) obtained after centrifugation of blood at 2,000 g for 2–4 minutes was mixed with 1.4 times the volume of acetonitrile. After stirring with a vortex mixer, the sample was centrifuged at 2,000 g for 4 min and 1.5 mL of water was added to the supernatant plasma-acetonitrile mixture, which was then injected into a radio-HPLC system. Blood (2-4 mL) and plasma (0.7-1.5 mL) samples were counted in a NaI well-counter. The radio-HPLC system used consisted of an interface module (D-7000; Hitachi: Tokyo, Japan), a L-7100 pump (Hitachi), an injector (model 7125, with a 5.0-mL loop; Rheodyne: Cotati, USA) equipped with a μ -Bondapak C18 column (300 x 7.8 mm, 10 μm; Waters: New England, USA), and an ultraviolet absorption detector (L-7400, 254 nm; Hitachi) in series with a 150TR; Packard (housed in a shield of 50 mm thick lead) equipped with a 550 μ L flow cell. Acetonitrile (A) and ammonium formate (100 mM) (B) were used as the mobile phase at 6.0 mL/min, according to the following gradient: 0–4 min (A/B), 40:60 → 80:20 v/v; 4.1–6 min(A/B), 80:20 v/v; 8 min (A/B), 40:60 v/v. Peaks for radioactive compounds eluting from the column were integrated and their areas were expressed as a percentage of the sum of the areas of all detected radioactive compounds (decay-corrected to the time of injection on the HPLC).

The free fraction, $f_p = C_{free} / C_{total}$, of [$^{11}$C]PBR28 in plasma was estimated using an ultrafiltration (Centrifree YM-30, Millipore) method. Equal amounts of [$^{11}$C]PBR28 were added to both plasma and phosphate buffered saline (control solution) and the radioactivity was counted with a NaI well-counter before ($C_{total}$) and after ultrafiltration ($C_{free}$). Results were corrected for the membrane binding measured with the control samples. For each PET examination a mean $f_p$ value was calculated based on 6 measurements.

## Image analysis

*Image pre-processing*

T1-weighted MR images were reoriented so that the line between the anterior and posterior commissure was in the horizontal plane and the interhemispheric fissure in the sagittal plane. MR images were segmented into grey and white matter and cerebrospinal fluid using the SPM5 segmentation algorithm in MATLAB (Wellcome Trust Centre for Neuroimaging, London, UK; The Mathworks, Natick, MA).

PET images were corrected for head movement by using a frame-by-frame realignment algorithm, in which all frames were individually realigned to the first minute of acquisition. The 4D PET images were integrated over time to obtain 3D PET summation images, and the re-oriented MRIs were then co-registered to the 3D PET summation images, yielding parameters of rotation and translation. The spatial processing of MR and PET images was performed in SPM5.

*ROI definition*

Regions of interest (ROIs) were obtained using the Automated Anatomical Labelling system [22] in SPM5 and applied to the dynamic PET image using coregistration parameters to create time activity curves (TACs). The primary ROI was brain gray matter (GM). In addition we quantified regional binding in thalamus (THA), putamen (PUT), hippocampus (HIP), lateral frontal cortex (LFC) and lateral temporal cortex (LTC), which all are regions of interest in research on the role of immune activation in neuropsychiatric disorders. Furthermore, a composite volume was created also for white matter (WM).

*Metabolite corrected arterial plasma input function*

Pre-processing of arterial blood data was performed using Kaleidagraph 4.1 software (Synergy Software). At first, dispersion correction was performed. Arterial blood data from the manual samplings were then linearly interpolated to obtain curves with one data point per second up to the end of PET acquisition. Blood time-activity curves were generated by integrating the initial automated blood sampling system curve with the

interpolated curve from manual blood samples. Plasma and blood radioactivity concentrations from manual blood samplings were divided to obtain a time curve for the plasma to blood ratio for the first five minutes. The first five minutes of the blood curve was then multiplied with the plasma/blood ratio curve to obtain an estimate for the plasma curve. The remaining part of the plasma curve was generated by linear interpolation, using the discrete direct plasma measurements. Correction for radioligand metabolism was performed in PMOD v3.2 (pixel-wise modelling software; PMOD Technologies Ltd., Zurich, Switzerland) using the parent fraction. Individual parent fraction data were fitted using a 3-exponential model.

*Quantification of [$^{11}$C]PBR28 binding*

For the main analysis of reproducibility, [$^{11}$C]PBR28 binding was quantified using the 2-tissue compartment model (2TCM) with a metabolite-corrected arterial plasma curve as input function using PMOD v3.2 software. In addition, [$^{11}$C]PBR28 binding was estimated using a voxel-by-voxel approach based on parametric images. Since $V_T$ has been shown to increase over time [9], and since shorter examination time would be beneficial in clinical studies, analyses were made for both 91 and 63 minutes of acquisition time. Finally, Standardized Uptake Values (SUV) were calculated for gray matter (GM) and plasma to assess the contribution of variance from brain and plasma measurements respectively.

*The 2-tissue compartment model (2TCM)*

The two tissue compartments are defined as the radioactivity concentration of non-displaceable radioligand in the brain ($C_{ND}$) and the radioactivity concentration of radioligand specifically bound to receptors ($C_S$). In this model, four rate constants ($K_1$, $k_2$, $k_3$ and $k_4$) are used to interpret the regional time curves for the radioligand in the brain. This model has previously been shown to be suitable for quantification of [$^{11}$C]PBR28 binding [9].

The rate constants were estimated by curve fitting using a least-squares approach. The blood volume fraction was set to a fixed value of 5 %. Regional [$^{11}$C]PBR28 binding was expressed as total volume of distribution ($V_T$), which is the sum of both specific and non-displaceable binding [23]. $V_T$ equals the ratio at steady state of the concentration of radioligand in brain to that in plasma, and can be calculated according to the following equation

$$V_T = \frac{K_1}{k_2} \cdot \left(1 + \frac{k_3}{k_4}\right) \quad (1)$$

*Parametric images*

Parametric images were generated using the wavelet aided parametric imaging (WAPI) method, with the stationary wavelet transform based parametric mapping framework implemented in Matlab R2007b for Windows [24]. The original dynamic PET images were transformed frame-by-frame to the wavelet space using a three-dimensional stationary wavelet transform in an iterative process which separates the high spatial frequencies from the low, using wavelet decomposition filters with finite support. The high frequency component is retained, whereas the low frequency component is separated at the next iteration into high and low frequencies using filters with a different cut-off frequency. The parameters of filter kernel (length of the wavelet filters) and depth-of-decomposition (optimal number of iterations) have previously been optimized to 16 and 3, respectively [25]. Quantification was performed with Logan's graphical analysis using multi-linear regression to fit the linear part of the curve of the coefficients from the dynamic wavelet transform [26]. The parametric wavelet transform describing the distribution of the total distribution volume ($V_T$) was then transformed to a three-dimensional (3D) parametric map of $V_T$ in normal space. The analysis was based on the last 60 minutes (for the 91 minute acquisition) and 36 minutes (63 minutes acquisition) respectively. The GM ROI was then applied to the WAPI images, to enable a comparison to the $V_T$ obtained using the 2TCM.

*Radioligand uptake in brain and plasma*

Standardized uptake values (SUV) were calculated for [$^{11}$C]PBR28 in GM and plasma by normalizing radioactivity measures to subject weight and injected radioactivity. The area under the curve (AUC) was then calculated for the whole time frame of the measurements.

## Statistics

The absolute variability, V, was expressed as the difference in $V_T$ between PET 1 and 2, relative to the mean of the two values according to the following equation:

$$V = \frac{ABS(V_{TPET1} - V_{TPET2})}{\frac{1}{2}(V_{TPET1} + V_{TPET2})} \cdot 100 \quad (2)$$

The intraclass correlation coefficient (ICC) is a measure of reliability, as indicated by the proportion of the variability in the data that is attributable to differences between methods, for instance between test and retest measurements. ICC ranges between 0 and 1, where values close to 1 indicates that the dominating proportion of the variability originates from variation between subjects. The ICC was calculated according to the following:

$$ICC = \frac{MSS_{subj} - MSS_{error}}{MSS_{subj}(k-1)MSS_{error} + \frac{k}{n}(MSS_{meth} - MSS_{error})}, \quad (3)$$

This version of ICC has been defined as ICC (A,1) by McGraw and Wong (1996). In the equation above, *k* and *n* denote the number of observations and subjects respectively and $MSS_{subj}$, $MSS_{meth}$, and $MSS_{error}$ denote the mean sum of squares for the subjects, the methods, and for the residual error.

To assess direction of change between PET1 and PET2, the difference in $V_T$ between the two measurements relative to the $V_T$ of PET 1 (*D*), was calculated as follows:

$$D = \frac{(V_{TPET2} - V_{TPET1})}{V_{TPET1}} \cdot 100 \quad (4)$$

The effect of gender and genotype on the reproducibility of [$^{11}$C]PBR28 binding was assessed using the Mann-Whitney U test. Differences between methods of quantification, as well as injected radioactivity and mass between PET 1 and PET 2 for all subjects, were tested using a paired t-test. Differences between morning and afternoon [$^{11}$C]PBR28 binding measures in the subgroup of 6 subjects, as well as differences in injected radioactivity, specific radioactivity and injected mass in the two subgroups, were tested using a Related Samples Wilcoxon Signed Rank Test. Statistical analyses were performed in IBM SPSS Statistics 22 (Armonk, NY, USA).

In addition, absolute variability according to equation (2) was calculated on a voxel-by-voxel basis using WAPI parametric images and a batch image calculator for SPM (http://tools.robjellis.net). For that purpose, parametric images were spatially normalized using the transformation matrix obtained in the above analyses, followed by smoothing with an 8 mm FWHM isotropic Gaussian kernel.

# Results

Following intravenous injection, [$^{11}$C]PBR28 appeared rapidly in brain and was homogenously distributed across all brain regions (Figure 1). Twelve subjects underwent two PET measurements according to the protocol, except for one individual where data acquisition was limited to 60 minutes for PET2. The values derived from this single examination were carried forward to the 63 and 91 minutes analyses. Mean injected radioactivity for PET1 and PET2 was 379 ± 61 and 410 ± 37 MBq, respectively (Table 1). This difference was statistically significant (p = 0.046). When examining the two different groups, a difference was found only in the group examined on different days (357 ± 75 vs. 417 ± 33 MBq, p=0.028). Mean injected mass also showed a difference, with higher levels for PET2 (0.53 ± 0.26 and 0.61 ± 0.3, respectively, p = 0.041). There was no statistical difference in injected mass between PET1 and PET2 in either of the two subgroups.

## Reproducibility in radioligand uptake and free fraction in plasma

The absolute variability for [$^{11}$C]PBR28 uptake in GM was 14.6 %, whereas the corresponding variability in plasma was 17.4%. The change in GM SUV AUC between PET1 and PET2 for the group examined on the same day was not statistically significant. In contrast, a 22.4 % decrease in plasma SUV was observed (p=0.028). The absolute variability of $f_p$ was 23.9 ± 13%.

## Reproducibility of $V_T$ : 2TCM

$V_T$ for gray matter (GM) calculated using 2TCM was the primary endpoint in the present analysis of reproducibility. The individual $V_T$ for GM varied between 1.3 and 7.8 (Figure 2, Table 1). The differences between PET1 and PET2 in $V_T$ (2TCM) for all brain regions are shown in Table 2. The absolute variability of $V_T$ in GM was 18.3 ± 12.7 %. The regional ICC values ranged from 0.90 to 0.94, except for WM (0.32), a region for which also the interindividual variability was high (48.3 ± 39.8 %). When calculating GM $V_T$ ICC for genetic groups separately, the values were 0.89 for HABs and 0.91 for MABs. Reducing the time of analysis to 63 minutes yielded similar values for the variability in $V_T$ (16.9 ± 14.9%) (Table 3). Although the absolute variation was numerically lower in the group examined on separate days, as compared to the ones examined on the same day (15.9 ± 12.2 vs. 20.7 ± 20.7), this difference was not significant (p=0.59). The difference in GM $V_T$ between morning and afternoon examinations in the group examined on the same day was not significant for the 91 minute analysis (p=0.116), whereas a significant difference was obtained for the 63 minute analysis (p=0.028).

## Effect of genotype on [$^{11}$C]PBR28 binding and reproducibility

The regional $V_T$ for gray matter (GM), quantified by 2TCM, for each subject and PET examination is shown in Table 1. The HAB subgroup showed an average GM $V_T$ value of 4.3 ± 1.8, for both measurements combined. In MABs the corresponding value was lower, 2.6 ± 1.1. In the HAB group there was one subject who presented markedly higher $V_T$ values (7.7 and 7.8 for PET1 and PET2 respectively). The regional $V_T$ values (2TCM) for the group examined on the same day, for the ones examined on separate days, as well as the mean of all subjects, are shown in Table 2. There was no effect of genotype on absolute variability (17.6% for MAB vs 19.1% for HAB; $p$=1.00).

## Parametric images

$V_T$ in gray matter (GM) in all individuals, as quantified with wavelet aided parametric imaging (WAPI), ranged between 1.3 and 7.7. There was a high degree of correlation to 2TCM-derived values (r=0.989, p<<0.001, all GM values combined (n=24)). The absolute variability of $V_T$ in GM, as derived from WAPI, was 17.8 % ± 12.7 (Table 3.). The mean difference in absolute variability between the two methods of quantification, 2TCM and WAPI, was 0.6% ± 9.0% (SD) (p=0.838). For WAPI-generated GM $V_T$ values, the difference between morning and afternoon examinations was statistically significant both for the 91 and 63 minute analyses (p=0.028). Colour-coded maps of voxel-wise absolute variability are shown in Figure 3. In accord with the ROI analysis, absolute variability in GM regions was in the range of 5-25%, whereas in WM regions values were above 30%. There were no GM regions with particularly high or low variability.

# Discussion

In this PET study we examined the test-retest reproducibility of [$^{11}$C]PBR28 in twelve healthy control subjects, by determining the regional volume of distribution of radioligand binding ($V_T$) in two consecutive PET examinations. The mean absolute variability in [$^{11}$C]PBR28 binding in gray matter regions ranged from 13.8 to 25.9 % depending on the region examined and the method of quantification used, and whether or not diurnal changes was controlled for. The reliability was high, with ICC values for $V_T$ in all GM regions ranging from 0.90 to 0.94. The reproducibility was at the same level when using a voxel-based quantification approach. Furthermore, reducing the time of analysis to 63 minutes did not increase variability.

[$^{11}$C]PBR28 is one among several more recently developed TSPO radioligands, designed to overcome the drawbacks of [$^{11}$C]PK11195. Information on test-retest reproducibility of a radioligand is important for interpreting clinical studies, both in longitudinal designs and when examining between-group differences. . To date, there is only one published test-retest reproducibility study of TSPO binding, using [$^{11}$C]PK11195 in six

healthy male control subjects [6]. In this study examinations were performed on average six weeks apart. In order to compare the results with the present study, we calculated the mean absolute variability based on the reported rate constants, and found it to be 15.9 % for $V_T$ in GM. The absolute variability in GM binding for both radioligands is thus well comparable. In contrast, the ICC value for GM was much lower (0.47) for [$^{11}$C]PK11195. Furthermore, in specific brain regions, the mean difference in *BP* for [$^{11}$C]PK11195 was substantially higher than the regional differences in $V_T$ in the present study, and ICC values were very low (ranging from negative values to 0.57). Although there were some differences in study design, including the use of different outcome measures of radioligand binding, the present analysis suggests that [$^{11}$C]PBR28 is more reliable for measurements of TSPO levels, in particular at an anatomically detailed level.

A mathematical explanation for the apparent discrepancy of high variability and high ICC values when comparing [$^{11}$C]PBR28 and [$^{11}$C]PK11195 is the substantially higher intersubject variability in the present sample. While the coefficient of variation (CoV) for GM was on average 25% in the previous analysis of [$^{11}$C]PK11195 [6], it was 49 % in the present study. When removing the individual with very high $V_T$ values, the variability was 36%. This range of intersubject variability is well in line with other [$^{11}$C]PBR28 studies in healthy subjects, using 2TCM and $V_T$ as outcome [9,27,28].

Approximately ten percent of humans lack specific binding of [$^{11}$C]PBR28 to TSPO [10], depending on a specific polymorphism in the TSPO gene [17]. This variation in binding affinity is a shared feature of all tested second generation TSPO ligands, as shown by *in vitro* studies [17]. In this study we confirmed previous findings of an effect of genotype on [$^{11}$C]PBR28 binding *in vivo*. The $V_T$ in high- affinity binders was approximately 65% higher than that of mixed affinity binders (2TCM). This difference is larger than what was found in recent studies on Standardized Uptake Values (30 % difference, [29]) and $V_T$ (30-40 % difference [30,31], although the discrepancy was highly influenced by the outlier individual in the HAB group. Importantly, we could not show an effect of genotype on test-retest reproducibility, suggesting that genotype does not have to be controlled for in clinical studies with a within-subject experimental design.

Apart from the effect of TSPO genotype, the relatively high intra- and interindividual variance in [$^{11}$C]PBR28 binding may be influenced by biological factors related to TSPO as a target, in addition to random noise. It is known that the amount of specific immune cells, such as monocytes, neutrophils and lymphocytes as well as cytokines show a 24-hour variation in plasma [32]. For instance, circadian changes in the levels of IL-6 have recently been demonstrated in both plasma and CSF of healthy controls [33]. The observation that cytokines have been shown to increase TSPO levels [2], attracts attention to diurnal changes in TSPO radioligand binding. In this study, there was no difference in the variability of $V_T$ between individuals examined at the same time of day and the group that was examined in the morning and afternoon. However, there was a trend-level increase in the main outcome measure of 2TCM-based GM $V_T$ between morning and afternoon measurements, and significant increases in WAPI-based and 63 minute 2TCM GM $V_T$ values. Moreover, a significant decrease was shown in plasma AUC. Although these preliminary findings in a limited sample cannot be regarded as conclusive, diurnal changes in TSPO binding may potentially be a confounder in clinical studies and the issue thus warrants further investigation.

When comparing a ROI-based compartmental analysis to a voxel-based quantification approach, the reproducibility values were in agreement. This may be of interest for clinical studies, since changes in the immune system in neuropsychiatric disorders may not follow anatomical boundaries [13]. A parametric approach for the analysis of TSPO binding may thus be a useful addition. Furthermore, variability remained unchanged when reducing the time of analysis from 91 to 63 minutes. This observation suggests that a shorter time frame for data acquisition may be used, in particular for clinical populations where long scanning times may present a practical problem.

As for all other TSPO radioligands, quantification of binding is dependent on the use of a metabolite-corrected arterial input function. The reason is that there is no brain region devoid of TSPO that can be used as reference, as has been confirmed in a recent blocking study [31]. The use of blood data increases the potential

methodological sources of variance, since several analysis steps are introduced. In particular, [$^{11}$C]PBR28 shows a rapid metabolism, resulting in low levels of parent compound remaining at end of the examination. Thus, even small errors introduced at this stage may propagate to having an effect on $V_T$. In the present study, variability in plasma was at the same level as the variability in GM uptake. Assuming that part of this variation is methodologically determined, this suggests that reproducibility could be further improved if this component of the analysis is removed. An important aim for future research will therefore be to investigate methods for [$^{11}$C]PBR28 quantification without the need of arterial blood sampling, such as the use of an image-derived input function [34] in relation to test-retest reproducibility.

## Conclusions

In the present study we found a low to medium reproducibility but high reliability of [$^{11}$C]PBR28 binding, irrespective of the method of quantification used. The results suggest that the radioligand is suitable for both within-subject and group comparisons, and that an examination length of 63 minutes could be sufficient for clinical studies. Furthermore, parametric approaches may be used to enable quantification of TSPO binding independent of anatomical ROI definition. Finally, if our preliminary findings on diurnal changes in measures of TSPO availability can be confirmed, this would necessitate controlling for time of examination in clinical studies.


## Acknowledgement

The research leading to these results has received funding from the Swedish Research Council (VR 09114), the European Union's Seventh Framework Programme (FP7/2007-2013) under grant agreement n$^{o}$ HEALTH-F2-2011-278850 (INMIND), Karolinska Institutet and PRIMA Barn och vuxenpsykiatri AB. I.Y.s contribution was supported by MINDVIEW: Multimodal Imaging of Neurological Disorders (Project reference: 603002); European comission's framework programme FP7-HEALTH.

We thank Ruyji Nakao for his diligent work with metabolite analyses, and Martin Schain for his generous help in calculating the ICCs. We also thank the other members of the PET group for their close assistance during this study.


## Conflicts of interest

L.F. is partially employed at the AstraZeneca Translational Science Center at Karolinska Institutet. S.C. has received grant support from AstraZeneca as co-investigator, and has served as a one-off speaker for Roche and Otsuka pharmaceuticals. A.V. has received funding from CHDI Foundations Inc. All other authors declare that they have no conflict of interest.

## Compliance with ethical standards

All procedures performed in studies involving human participants were in accordance with the ethical standards of the institutional and/or national research committee and with the 1964 Helsinki declaration and its later amendments or comparable ethical standards. Informed consent was obtained from all individual participants included in the study.

## References


1. Raivich G. Like cops on the beat: the active role of resting microglia. Trends Neurosci. [Internet]. 2005 [cited 2013 Mar 22];28:571–3. Available from: http://www.ncbi.nlm.nih.gov/pubmed/16165228

2. Venneti S, Lopresti BJ, Wiley CA. The peripheral benzodiazepine receptor (Translocator protein 18kDa) in microglia: from pathology to imaging. Prog. Neurobiol. [Internet]. 2006 [cited 2013 Mar 13];80:308–22. Available from: http://www.pubmedcentral.nih.gov/articlerender.fcgi?artid=1849976&tool=pmcentrez&rendertype=abstract

3. Papadopoulos V, Baraldi M, Guilarte TR, Knudsen TB, Lacapère J-J, Lindemann P, et al. Translocator protein (18kDa): new nomenclature for the peripheral-type benzodiazepine receptor based on its structure and molecular function. Trends Pharmacol. Sci. [Internet]. 2006 [cited 2013 Apr 16];27:402–9. Available from: http://www.ncbi.nlm.nih.gov/pubmed/16822554

4. Cagnin A, Kassiou M, Meikle SR, Banati RB. Positron emission tomography imaging of neuroinflammation. Neurotherapeutics [Internet]. 2007 [cited 2013 Apr 16];4:443–52. Available from: http://www.ncbi.nlm.nih.gov/pubmed/17599710

5. Imaizumi M, Briard E, Zoghbi SS, Gourley JP, Hong J, Fujimura Y, et al. Brain and whole-body imaging in nonhuman primates of [11C]PBR28, a promising PET radioligand for peripheral benzodiazepine receptors. Neuroimage [Internet]. 2008 [cited 2013 Apr 16];39:1289–98. Available from: http://www.pubmedcentral.nih.gov/articlerender.fcgi?artid=2275117&tool=pmcentrez&rendertype=abstract

6. Jučaite A, Cselényi Z, Arvidsson A, Ahlberg G, Julin P, Varnäs K, et al. Kinetic analysis and test-retest variability of the radioligand [11C](R)-PK11195 binding to TSPO in the human brain - a PET study in control subjects. EJNMMI Res. [Internet]. Springer Open Ltd; 2012 [cited 2013 Apr 5];2:15. Available from: http://www.pubmedcentral.nih.gov/articlerender.fcgi?artid=3350394&tool=pmcentrez&rendertype=abstract

7. Hirvonen J, Aalto S, Lumme V, Någren K, Kajander J, Vilkman H, et al. Measurement of striatal and thalamic dopamine D2 receptor binding with 11C-raclopride. Nucl. Med. Commun. [Internet]. 2003 [cited 2013 Apr 15];24:1207–14. Available from: http://www.ncbi.nlm.nih.gov/pubmed/14627846

8. Owen DRJ, Matthews PM. Imaging brain microglial activation using positron emission tomography and translocator protein-specific radioligands. Int. Rev. Neurobiol. [Internet]. 2011 [cited 2013 Apr 16];101:19–39. Available from: http://www.ncbi.nlm.nih.gov/pubmed/22050847

9. Fujita M, Imaizumi M, Zoghbi SS, Fujimura Y, Farris AG, Suhara T, et al. Kinetic analysis in healthy humans of a novel positron emission tomography radioligand to image the peripheral benzodiazepine receptor, a potential biomarker for inflammation. Neuroimage [Internet]. 2008 [cited 2013 Apr 16];40:43–52. Available from: http://www.pubmedcentral.nih.gov/articlerender.fcgi?artid=2265774&tool=pmcentrez&rendertype=abstract

10. Kreisl WC, Fujita M, Fujimura Y, Kimura N, Jenko KJ, Kannan P, et al. Comparison of [11C]-(R)-PK 11195 and [11C]PBR28, two radioligands for translocator protein (18 kDa) in human and monkey: Implications for positron emission tomographic imaging of this inflammation biomarker. Neuroimage [Internet]. 2010 [cited 2013 Dec 2];49:2924–32. Available from: http://www.sciencedirect.com/science/article/pii/S1053811909012427

11. Hannestad J, Gallezot J-D, Schafbauer T, Lim K, Kloczynski T, Morris ED, et al. Endotoxin-induced systemic inflammation activates microglia: [$^{11}$C]PBR28 positron emission tomography in nonhuman primates. Neuroimage [Internet]. Elsevier Inc.; 2012 [cited 2013 Apr 5];63:232–9. Available from: http://www.ncbi.nlm.nih.gov/pubmed/22776451

12. Kreisl WC, Lyoo CH, McGwier M, Snow J, Jenko KJ, Kimura N, et al. In vivo radioligand binding to translocator protein correlates with severity of Alzheimer's disease. Brain [Internet]. 2013 [cited 2014 Jun 7];136:2228–38. Available from: http://www.ncbi.nlm.nih.gov/pubmed/23775979

13. Oh U, Fujita M, Ikonomidou VN, Evangelou IE, Matsuura E, Harberts E, et al. Translocator protein PET imaging for glial activation in multiple sclerosis. J. Neuroimmune Pharmacol. [Internet]. 2011 [cited 2014 Nov 25];6:354–61. Available from: http://www.pubmedcentral.nih.gov/articlerender.fcgi?artid=3257858&tool=pmcentrez&rendertype=abstract

14. Fujita M, Mahanty S, Zoghbi SS, Ferraris Araneta MD, Hong J, Pike VW, et al. PET reveals inflammation around calcified Taenia solium granulomas with perilesional edema. PLoS One [Internet]. 2013 [cited 2014 Nov 25];8:e74052. Available from: http://www.pubmedcentral.nih.gov/articlerender.fcgi?artid=3773048&tool=pmcentrez&rendertype=abstract

15. Nakao A. Temporal regulation of cytokines by the circadian clock. J. Immunol. Res. [Internet]. Hindawi Publishing Corporation; 2014 [cited 2014 Nov 7];2014:614529. Available from: /pmc/articles/PMC3997878/?report=abstract

16. Curtis AM, Bellet MM, Sassone-Corsi P, O'Neill LAJ. Circadian clock proteins and immunity. Immunity [Internet]. 2014 [cited 2014 Oct 27];40:178–86. Available from: http://www.sciencedirect.com/science/article/pii/S1074761314000405

17. Owen DR, Yeo AJ, Gunn RN, Song K, Wadsworth G, Lewis A, et al. An 18-kDa translocator protein (TSPO) polymorphism explains differences in binding affinity of the PET radioligand PBR28. J. Cereb. Blood Flow Metab. [Internet]. Nature Publishing Group; 2012 [cited 2013 Feb 27];32:1–5. Available from: http://www.pubmedcentral.nih.gov/articlerender.fcgi?artid=3323305&tool=pmcentrez&rendertype=abstract

18. Briard E, Zoghbi SS, Imaizumi M, Gourley JP, Shetty HU, Hong J, et al. Synthesis and evaluation in monkey of two sensitive 11C-labeled aryloxyanilide ligands for imaging brain peripheral benzodiazepine receptors in vivo. J. Med. Chem. [Internet]. American Chemical Society; 2008 [cited 2014 Nov 25];51:17–30. Available from: http://pubs.acs.org.proxy.kib.ki.se/doi/abs/10.1021/jm0707370

19. Bergström M, Boëthius J, Eriksson L, Greitz T, Ribbe T, Widén L. Head fixation device for reproducible position alignment in transmission CT and positron emission tomography. J. Comput. Assist. Tomogr. [Internet]. 1981 [cited 2013 Apr 25];5:136–41. Available from: http://www.ncbi.nlm.nih.gov/pubmed/6972391

20. Varrone A, Sjöholm N, Eriksson L, Gulyás B, Halldin C, Farde L. Advancement in PET quantification using 3D-OP-OSEM point spread function reconstruction with the HRRT. Eur. J. Nucl. Med. Mol. Imaging [Internet]. 2009 [cited 2013 Apr 25];36:1639–50. Available from: http://www.ncbi.nlm.nih.gov/pubmed/19437012

21. Farde L, Eriksson L, Blomquist G, Halldin C. Kinetic analysis of central [11C]raclopride binding to D2-dopamine receptors studied by PET--a comparison to the equilibrium analysis. J. Cereb. Blood Flow Metab. [Internet]. 1989 [cited 2015 Jan 1];9:696–708. Available from: http://www.ncbi.nlm.nih.gov/pubmed/2528555

22. Tzourio-Mazoyer N, Landeau B, Papathanassiou D, Crivello F, Etard O, Delcroix N, et al. Automated anatomical labeling of activations in SPM using a macroscopic anatomical parcellation of the MNI MRI single-subject brain. Neuroimage [Internet]. 2002 [cited 2014 Jul 10];15:273–89. Available from: http://www.sciencedirect.com/science/article/pii/S1053811901909784

23. Innis RB, Cunningham VJ, Delforge J, Fujita M, Gjedde A, Gunn RN, et al. Consensus nomenclature for in vivo imaging of reversibly binding radioligands. J. Cereb. Blood Flow Metab. [Internet]. 2007 [cited 2014 Jul 16];27:1533–9. Available from: http://www.ncbi.nlm.nih.gov/pubmed/17519979

24. Cselényi Z, Olsson H, Halldin C, Gulyás B, Farde L. A comparison of recent parametric neuroreceptor mapping approaches based on measurements with the high affinity PET radioligands [11C]FLB 457 and [11C]WAY 100635. Neuroimage [Internet]. 2006 [cited 2014 Dec 15];32:1690–708. Available from: http://www.ncbi.nlm.nih.gov/pubmed/16859930

25. Schain M, Tóth M, Cselényi Z, Arakawa R, Halldin C, Farde L, et al. Improved mapping and quantification of serotonin transporter availability in the human brainstem with the HRRT. Eur. J. Nucl. Med. Mol. Imaging [Internet]. 2013 [cited 2015 May 18];40:228–37. Available from: http://www.ncbi.nlm.nih.gov/pubmed/23076621

26. Turkheimer FE, Aston JAD, Banati RB, Riddell C, Cunningham VJ. A linear wavelet filter for parametric imaging with dynamic PET. IEEE Trans. Med. Imaging [Internet]. 2003 [cited 2015 May 18];22:289–301. Available from: http://www.ncbi.nlm.nih.gov/pubmed/12760547

27. Narendran R, Lopresti BJ, Mason NS, Deuitch L, Paris J, Himes ML, et al. Cocaine abuse in humans is not associated with increased microglial activation: an 18-kDa translocator protein positron emission tomography imaging study with [11C]PBR28. J. Neurosci. [Internet]. 2014 [cited 2014 Dec 1];34:9945–50. Available from: http://www.ncbi.nlm.nih.gov/pubmed/25057196

28. Kreisl WC, Jenko KJ, Hines CS, Hyoung Lyoo C, Corona W, Morse CL, et al. A genetic polymorphism for translocator protein 18 kDa affects both in vitro and in vivo radioligand binding in human brain to this putative biomarker of neuroinflammation. J. Cereb. Blood Flow Metab. 2012.

29. Yoder KK, Nho K, Risacher SL, Kim S, Shen L, Saykin AJ. Influence of TSPO genotype on 11C-PBR28 standardized uptake values. J. Nucl. Med. [Internet]. 2013 [cited 2014 Nov 25];54:1320–2. Available from: http://www.pubmedcentral.nih.gov/articlerender.fcgi?artid=3740346&tool=pmcentrez&rendertype=abstract

30. Kreisl WC, Jenko KJ, Hines CS, Lyoo CH, Corona W, Morse CL, et al. A genetic polymorphism for translocator protein 18 kDa affects both in vitro and in vivo radioligand binding in human brain to this putative biomarker of neuroinflammation. J. Cereb. Blood Flow Metab. [Internet]. 2013 [cited 2014 Nov 25];33:53–8. Available from: http://www.pubmedcentral.nih.gov/articlerender.fcgi?artid=3597372&tool=pmcentrez&rendertype=abstract

31. Owen DR, Guo Q, Kalk NJ, Colasanti A, Kalogiannopoulou D, Dimber R, et al. Determination of [(11)C]PBR28 binding potential in vivo: a first human TSPO blocking study. J. Cereb. Blood Flow Metab. [Internet]. Nature Publishing Group; 2014 [cited 2014 Nov 25];34:989–94. Available from: http://www.ncbi.nlm.nih.gov/pubmed/24643083

32. Haus E, Smolensky MH. Biologic rhythms in the immune system. Chronobiol. Int. [Internet]. 1999 [cited 2014 Nov 25];16:581–622. Available from: http://www.ncbi.nlm.nih.gov/pubmed/10513884

33. Agorastos A, Hauger RL, Barkauskas DA, Moeller-Bertram T, Clopton PL, Haji U, et al. Circadian rhythmicity, variability and correlation of interleukin-6 levels in plasma and cerebrospinal fluid of healthy men. Psychoneuroendocrinology [Internet]. 2014 [cited 2014 Nov 25];44:71–82. Available from: http://www.ncbi.nlm.nih.gov/pubmed/24767621

34. Schain M, Benjaminsson S, Varnäs K, Forsberg A, Halldin C, Lansner A, et al. Arterial input function derived from pairwise correlations between PET-image voxels. J. Cereb. Blood Flow Metab. [Internet]. 2013 [cited 2014 Dec 9];33:1058–65. Available from: http://www.pubmedcentral.nih.gov/articlerender.fcgi?artid=3705432&tool=pmcentrez&rendertype=abstract

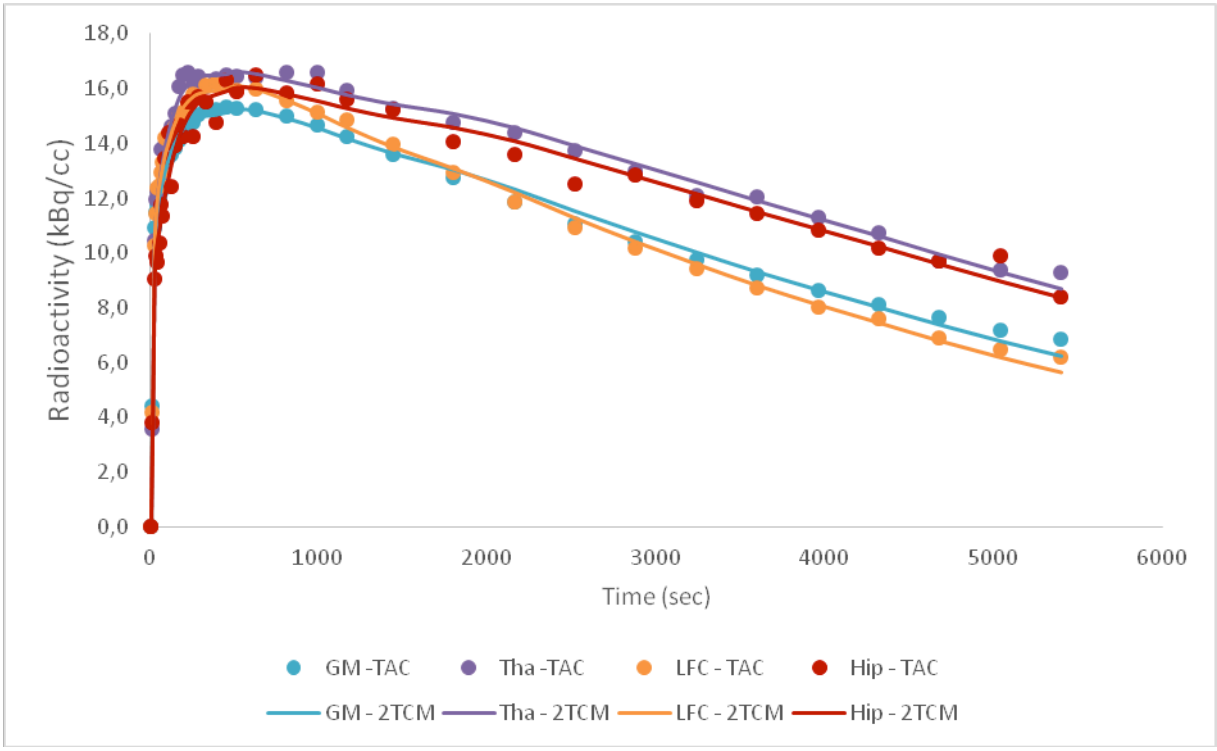


**Figure 1.** Representative figure showing data for subject 2. Two-tissue-compartment model fit to time–activity curves for Grey matter (GM), Thalamus (Tha), Lateral frontal cortex (LFC), and Hippocampus (Hip).

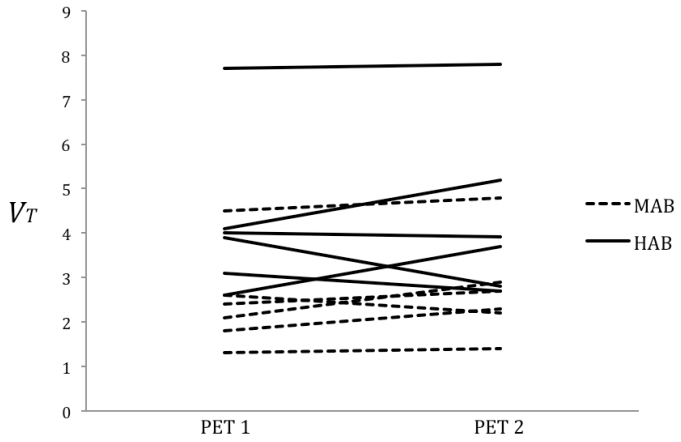


**Figure 2.** Line charts indicating change in [$^{11}$C]PBR28 volume of distribution ($V_T$) in gray matter between PET 1 and 2 for each subject, as derived from 2TCM.

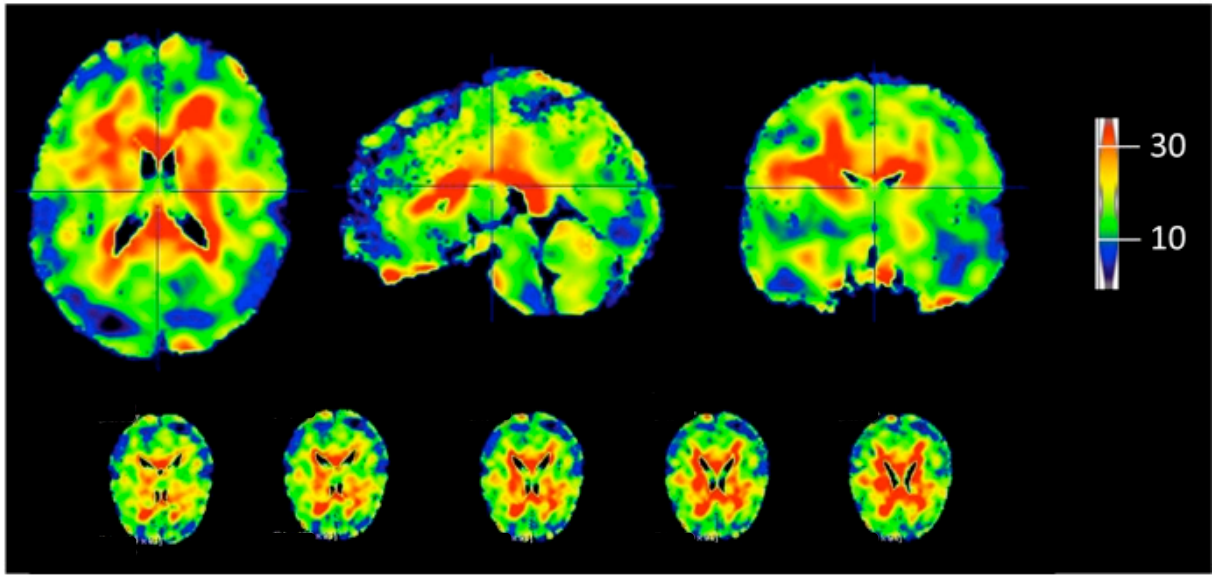
30
10

**Table 1**

Gender, age, genotype, time, injected radioactivity (MBq,) injected mass tracer (µg),

mean free fraction ($f_P$) and $V_T$ values in Gray Matter (GM) using two tissue compartment model (2TCM), for PET 1 and 2

| | | | | PET 1 | | | | | | PET 2 | | | | | |
|---|---|---|---|---|---|---|---|---|---|---|---|---|---|---|---|
| **Subject** | **Gender** | **Age** | **Genotype** | **Time** | **Injected radioactivity** | **Injected mass** | ***VT*** | ***$f_P$*** | ***SD ($f_P$)*** | **Time** | **Injected radioactivity** | **Injected mass** | ***VT*** | ***$f_P$*** | ***SD ($f_P$)*** |
| *Examinations on same day* | | | | | | | | | | | | | | | |
| 1 | F | 20 | MAB | 10:22 | 359 | 0,53 | 2,6 | 11,1 | 1,3 | 13:08 | 350 | 0,59 | 2,2 | 7,9 | 0,4 |
| 2 | F | 22 | HAB | 10:02 | 354 | 0,22 | 7,7 | 11,3 | 1,3 | 13:00 | 367 | 0,2 | 7,8 | 15,5 | 2,5 |
| 3 | M | 28 | MAB | 10:45 | 400 | 0,19 | 2,4 | 12,7 | 1,1 | 13:40 | 443 | 0,18 | 2,7 | 11,6 | 0,8 |
| 4 | M | 22 | HAB | 10:51 | 458 | 0,22 | 2,6 | 13,8 | 0,2 | 13:56 | 454 | 0,26 | 3,7 | 9,1 | 0,7 |
| 5 | F | 25 | MAB | 10:45 | 421 | 0,42 | 2,1 | 10,6 | 1,0 | 13:54 | 380 | 0,59 | 2,9 | 12,2 | 0,1 |
| 6 | M | 25 | HAB | 10:00 | 414 | 0,38 | 4,1 | 10,8 | 1,0 | 15:27 | 426 | 0,51 | 5,2 | 7,2 | 0,7 |
| *Examinations on different days* | | | | | | | | | | | | | | | |
| 7 | M | 27 | HAB | 10:04 | 439 | 0,62 | 3,9 | 7,0 | 0,1 | 11:10 | 462 | 0,62 | 2,8 | 5,3 | 0,0 |
| 8 | M | 23 | MAB | 09:59 | 418 | 0,89 | 1,3 | na | na | 10:12 | 447 | 0,94 | 1,4 | 7,4 | 0,9 |
| 9 | M | 29 | HAB | 09:54 | 248 | 0,86 | 4,0 | 7,9 | 0,5 | 09:59 | 394 | 0,75 | 3,9 | 6,1 | 0,2 |
| 10 | F | 20 | MAB | 09:56 | 300 | 0,7 | 1,8 | 5,3 | 0,1 | 10:07 | 375 | 0,97 | 2,3 | 5,2 | 0,4 |
| 11 | F | 21 | MAB | 10:08 | 335 | 0,89 | 4,5 | 7,8 | 0,2 | 09:49 | 406 | 1,12 | 4,8 | 6,0 | 0,3 |
| 12 | F | 25 | HAB | 09:57 | 400 | 0,48 | 3,1 | 9,2 | 0,3 | 09:58 | 420 | 0,55 | 2,7 | 8,1 | 0,0 |

**Table 2**

Regional TSPO binding as $V_T$ derived from 2TCM (91 min);
difference (%) and absolute variability (%) between PET 1 and 2

| Region | Same day | | Separate days | | Total | | |
|---|---|---|---|---|---|---|---|
| | mean (n=6) | SD | mean (n=6) | SD | mean (n=12) | SD | ICC |
| **Grey matter** | | | | | | | 0,92 |
| PET1 | 3,6 | 2,1 | 3,1 | 1,3 | 3,3 | 1,7 | |
| PET2 | 4,1 | 2,1 | 3,0 | 1,2 | 3,5 | 1,7 | |
| Difference (%) | 18,5 | 23,9 | 0,2 | 20,7 | 9,3 | 23,4 | |
| Absolute variability (%) | 20,7 | 13,8 | 15,9 | 12,2 | 18,3 | 12,7 | |
| **Thalamus** | | | | | | | 0,91 |
| PET1 | 4,4 | 3,1 | 3,9 | 1,9 | 4,1 | 2,5 | |
| PET2 | 5,2 | 2,8 | 3,6 | 1,9 | 4,4 | 2,4 | |
| Difference (%) | 27,4 | 25,9 | -2,5 | 31,5 | 12,4 | 31,6 | |
| Absolute variability (%) | 23,1 | 18,5 | 23,5 | 17,4 | 23,3 | 17,1 | |
| **Putamen** | | | | | | | 0,90 |
| PET1 | 3,6 | 2,2 | 3,2 | 1,2 | 3,4 | 1,7 | |
| PET2 | 4,0 | 2,2 | 2,9 | 1,4 | 3,5 | 1,8 | |
| Difference (%) | 15,9 | 31,1 | -8,4 | 19,2 | 3,7 | 27,7 | |
| Absolute variability (%) | 25,5 | 16,7 | 16,8 | 17,2 | 21,2 | 16,8 | |
| **Hippocampus** | | | | | | | 0,94 |
| PET1 | 4,4 | 2,9 | 3,5 | 1,6 | 3,9 | 2,3 | |
| PET2 | 4,9 | 2,8 | 3,3 | 1,6 | 4,1 | 2,4 | |
| Difference (%) | 15,3 | 16,5 | -1,1 | 24,3 | 7,1 | 21,6 | |
| Absolute variability (%) | 16,1 | 10,7 | 21,3 | 10,9 | 18,7 | 10,7 | |
| **Lateral frontal cortex** | | | | | | | 0,90 |
| PET1 | 3,4 | 2,0 | 3,2 | 1,2 | 3,3 | 1,6 | |
| PET2 | 3,9 | 2,1 | 3,1 | 1,2 | 3,5 | 1,7 | |
| Difference (%) | 19,5 | 31,6 | 0,7 | 19,4 | 10,1 | 26,8 | |
| Absolute variability (%) | 25,9 | 16,4 | 14,5 | 11,6 | 20,2 | 14,8 | |
| **Lateral temporal cortex** | | | | | | | 0,94 |
| PET1 | 3,7 | 2,2 | 3,1 | 1,4 | 3,4 | 1,7 | |
| PET2 | 4,1 | 2,1 | 3,0 | 1,2 | 3,6 | 1,7 | |
| Difference (%) | 14,3 | 21,9 | 0,9 | 19,2 | 7,6 | 20,9 | |
| Absolute variability (%) | 18,7 | 12,1 | 14,7 | 11,6 | 16,7 | 11,5 | |
| **White matter** | | | | | | | 0,32 |
| PET1 | 3,2 | 1,5 | 3,2 | 1,2 | 3,2 | 1,3 | |
| PET2 | 5,2 | 3,4 | 2,5 | 1,4 | 3,8 | 2,9 | |
| Difference (%) | 83,7 | 122,5 | -20,1 | 39,8 | 31,8 | 102,4 | |
| Absolute variability (%) | 51,4 | 44,4 | 45,2 | 38,5 | 48,3 | 39,8 | |

2TCM=two tissue compartment model; $V_T$=volume of distribution;
SD=standard deviation; ICC=intraclass correlation coefficiant

**Table 3**

Mean gray matter $V_T$ for PET 1 and 2, difference (%)
and absolute variability (%) for different methods of analysis as well as for free fraction ($f_P$)

| Method | Same day mean (n=6) | Separate days mean (n=6) | Total mean (n=12) | SD |
|---|---|---|---|---|
| **Brain radioactivity, AUC (SUV*min), 91 min** | | | | |
| PET1 | 6577 | 6150 | 6363 | 1398 |
| PET2 | 6077 | 5532 | 5805 | 1192 |
| Difference (%) | -7,6 | -7,4 | -7,5 | 14,7 |
| Absolute variability (%) | 12,6 | 15,6 | 14,6 | 9,5 |
| **Plasma radioactivity, AUC (SUV*min), 91 min** | | | | |
| PET1 | 2639 | 2706 | 2672 | 782 |
| PET2 | 1994 | 2441 | 2218 | 538 |
| Difference (%) | -22,4* | -8,1 | -15,3 | 11,6 |
| Absolute variability (%) | 25,9 | 8,8 | 17,4 | 13,9 |
| **2TCM 63 min** | | | | |
| PET1 | 3,3 | 2,9 | 3,1 | 1,7 |
| PET2 | 3,9 | 2,8 | 3,4 | 1,7 |
| Difference (%) | 24.1* | -0,8 | 11,7 | 23,6 |
| Absolute variability (%) | 20,0 | 13,8 | 16,9 | 14,9 |
| **WAPI 63 min** | | | | |
| PET1 | 3,2 | 2,7 | 2,9 | 1,7 |
| PET2 | 3,7 | 2,7 | 3,2 | 1,6 |
| Difference (%) | 24.9* | 4,8 | 14,8 | 22,0 |
| Absolute variability (%) | 21,4 | 16,2 | 18,8 | 13,5 |
| **WAPI 91 min** | | | | |
| PET1 | 3,3 | 2,8 | 3,1 | 1,8 |
| PET2 | 3,9 | 2,9 | 3,4 | 1,7 |
| Difference (%) | 24.1* | 6,9 | 15,5 | 20,5 |
| Absolute variability (%) | 20,8 | 14,7 | 17,8 | 12,7 |
| $f_P$ | | | | |
| PET1 | 11,7 | 7,4 | 9,8 | 2,6 |
| PET2 | 10,6 | 6,4 | 8,5 | 3,2 |
| Difference (%) | -8,7 | -16,5 | -12,2 | 22,3 |
| Absolute variability (%) | 28,4 | 18,5 | 23,9 | 13,0 |

2TCM=two tissue compartment model; $V_T$=volume of distribution;
WAPI=analysis based on waivelet-aided parametric images;
SD=standard deviation; SUV= standard uptake value
$f_P$ = free fraction
* = $p$<0.05

**Table 4**

Rate constants $k_1$, $k_2$, $k_3$, $k_4$ for PET 1 and 2, difference(%) and absolute variability (%)

| Rate constants | Same day mean | Separate days mean | Total mean | SD |
|---|---|---|---|---|
| $k_1$ | | | | |
| PET1 | 0,16 | 0,15 | 0,2 | 0,1 |
| PET2 | 0,17 | 0,16 | 0,16 | 0,05 |
| Difference (%) | 4,5 | 6,0 | 5,3 | 15,7 |
| Absolute variability (%) | 8,7 | 20,0 | 14,4 | 9,0 |
| $k_2$ | | | | |
| PET1 | 0,18 | 0,16 | 0,17 | 0,07 |
| PET2 | 0,16 | 0,25 | 0,21 | 0,13 |
| Difference (%) | -11,2 | 12,7 | 0,7 | 37,5 |
| Absolute variability (%) | 21,1 | 42,0 | 31,5 | 38,8 |
| $k_3$ | | | | |
| PET1 | 0,13 | 0,08 | 0,1 | 0,1 |
| PET2 | 0,16 | 0,16 | 0,2 | 0,1 |
| Difference (%) | 24,9 | 1,5 | 13,2 | 55,3 |
| Absolute variability (%) | 44,1 | 61,6 | 52,9 | 41,3 |
| $k_4$ | | | | |
| PET1 | 0,04 | 0,05 | 0,04 | 0,02 |
| PET2 | 0,05 | 0,05 | 0,1 | 0,02 |
| Difference (%) | 22,0 | 0,2 | 11,1 | 30,3 |
| Absolute variability (%) | 33,2 | 21,4 | 27,3 | 33,8 |
| $k_1/k_2$ | | | | |
| PET1 | 0,89 | 1,20 | 1,0 | 0,5 |
| PET2 | 1,00 | 1,03 | 1,0 | 0,5 |
| Difference (%) | 10,5 | -57,7 | -23,6 | 102,5 |
| Absolute variability (%) | 20,4 | 33,8 | 27,1 | 32,5 |
| $k_3/k_4$ | | | | |
| PET1 | 2,87 | 1,72 | 2,29 | 1,16 |
| PET2 | 2,95 | 2,71 | 2,83 | 1,56 |
| Difference (%) | -4,7 | 11,9 | 3,6 | 43,4 |
| Absolute variability (%) | 29,9 | 45,3 | 37,6 | 34,8 |

SD=standard deviation